

UC San Diego

UC San Diego Previously Published Works

Title

Cadm4 restricts the production of cardiac outflow tract progenitor cells.

Permalink

<https://escholarship.org/uc/item/4466p06k>

Journal

Cell Reports, 7(4)

Authors

Zeng, Xin-Xin

Yelon, Deborah

Publication Date

2014-05-22

DOI

10.1016/j.celrep.2014.04.013

Peer reviewed



Published in final edited form as:

Cell Rep. 2014 May 22; 7(4): 951–960. doi:10.1016/j.celrep.2014.04.013.

Cadm4 restricts the production of cardiac outflow tract progenitor cells

Xin-Xin I.Zeng and Deborah Yelon*

Division of Biological Sciences, University of California, San Diego, La Jolla, CA, 92093, USA

SUMMARY

Heart assembly requires input from two populations of progenitor cells – the first and second heart fields – that differentiate at distinct times and create different cardiac components. The cardiac outflow tract (OFT) is built through recruitment of late-differentiating, second heart field (SHF)-derived cardiomyocytes to the arterial pole of the heart. Mechanisms responsible for selection of an appropriate number of OFT cells from the SHF remain unclear. Here, we find that *cell adhesion molecule 4 (cadm4)* is essential for restricting the size of the zebrafish OFT. Knockdown of *cadm4* causes dramatic OFT expansion, and overexpression of *cadm4* results in a greatly diminished OFT. Moreover, *cadm4* activity limits the production of OFT progenitor cells and the duration of their accumulation at the arterial pole. Together, our data are the first to suggest a role for cell adhesion in restraining SHF deployment to the OFT, perturbation of which could cause congenital OFT defects.

INTRODUCTION

The vertebrate heart is built from two sources of cardiac progenitor cells – the first heart field (FHF) and second heart field (SHF) – that differ in their timing of differentiation and in their contributions to specific regions of the heart (Kelly, 2012). First, cardiomyocytes (CMs) arising from the FHF create the primitive heart tube. Later, the poles of this tube grow through the progressive recruitment of newly formed CMs that are derived from the SHF. The SHF serves as an integral reservoir of developmental potential, composed of proliferative progenitor cells poised to contribute to the heart when the timing is right (Hutson et al., 2010; Tirosh-Finkel et al., 2010; van den Berg et al., 2009). It is therefore important to understand the network of signals that control SHF deployment and insure that the appropriate populations differentiate in a timely fashion.

The cardiac outflow tract (OFT) is an example of a crucial SHF-derived structure: a correctly elongated, properly oriented, and accurately subdivided OFT is essential for effective connection of the heart to the vasculature. Since many cases of congenital heart

© 2014 Elsevier Inc. All rights reserved.

*Contact: yelon@ucsd.edu; Phone: (858) 534-1822.

Publisher's Disclaimer: This is a PDF file of an unedited manuscript that has been accepted for publication. As a service to our customers we are providing this early version of the manuscript. The manuscript will undergo copyediting, typesetting, and review of the resulting proof before it is published in its final citable form. Please note that during the production process errors may be discovered which could affect the content, and all legal disclaimers that apply to the journal pertain.

disease feature OFT malformations (Neeb et al., 2013), regulation of OFT dimensions has great clinical importance. OFT formation begins with assembly of a small tube of myocardium at the arterial pole of the heart (Buckingham et al., 2005; Dyer and Kirby, 2009a). This myocardial foundation is built by late-differentiating, SHF-derived progenitor cells that reside in pharyngeal mesoderm before recruitment into the OFT. Although the SHF origin of OFT CMs has been clearly established, precise molecular mechanisms responsible for generating the proper number of OFT CMs from this progenitor pool remain unclear.

Among pathways implicated in regulation of SHF development (Rochais et al., 2009), Fgf signaling has a central role in driving OFT CM formation. In the early embryo, Fgf signaling plays an integral part in heart field induction, counterbalanced by retinoic acid signaling that limits field dimensions (Ryckebusch et al., 2008; Sirbu et al., 2008; Sorrell and Waxman, 2011; Witzel et al., 2012). Later, Fgf signaling within the SHF regulates proliferation, survival, and deployment of OFT progenitor cells (Ilagan et al., 2006; Park et al., 2006; Park et al., 2008; Watanabe et al., 2010). Several other signals, including Hedgehog and Bmp (Dyer and Kirby, 2009b; Hami et al., 2011; Hutson et al., 2010; Prall et al., 2007; Tirosh-Finkel et al., 2010), collaborate with Fgf signaling to regulate OFT CM formation. However, the mechanisms that restrain production of OFT CMs from the SHF remain poorly understood.

Here, we show that the gene *cell adhesion molecule 4* (*cadm4*) has a potent role in restricting the size of the OFT. Members of the Cadm family of type I transmembrane proteins (also known as SynCAM, Tsl, Igsf4, or Necl proteins) contain three extracellular Ig-like domains, a single-pass transmembrane domain, and a short cytoplasmic domain with both 4.1B-binding and PDZ-binding interaction motifs (Biederer, 2006). Through heterophilic extracellular interactions between family members, Cadms are known to act as cell adhesion molecules in several contexts, including myelination and synaptogenesis (Biederer et al., 2002; Maurel et al., 2007; Spiegel et al., 2007), but the roles of Cadms during heart development have not been previously examined.

In zebrafish, we find that *cadm4* is expressed near the arterial pole, where SHF-derived OFT progenitor cells reside. Strikingly, loss of *cadm4* function causes dramatic enlargement of the OFT, whereas gain of *cadm4* function results in a diminished OFT. Alteration in the number of OFT CMs is preceded by alterations in the proliferation, accumulation, and perdurance of OFT progenitor cells, indicating an important function of *cadm4* in limiting recruitment of progenitors from the SHF to the arterial pole. Together, our results suggest a model in which modulation of *cadm4* function alters critical extracellular interactions that dictate the dynamics of SHF deployment, perturbation of which could cause congenital defects in OFT formation.

RESULTS

Fgf signaling promotes formation of OFT progenitor cells

To enhance our understanding of OFT size regulation, we sought to identify genes with a potent impact on production of OFT progenitor cells. Our prior studies have shown that Fgf

signaling plays an essential role in promoting formation of OFT CMs in zebrafish (de Pater et al., 2009), just as it does in amniotes (Ilagan et al., 2006; Park et al., 2006). Zebrafish *fgf8a* mutants exhibit a small ventricle and lack an evident OFT, and temporally controlled inhibition of Fgf signaling can dissociate two distinct roles of this pathway: an early requirement for the initial specification of ventricular progenitors and a later requirement for the production of OFT CMs (de Pater et al., 2009; Marques et al., 2008). Treatment with the Fgfr antagonist SU5402 from 24 hours post-fertilization (hpf) inhibits OFT formation (Fig. 1A,F) (de Pater et al., 2009). Moreover, absence of an evident OFT in SU5402-treated embryos is preceded by diminished expression of markers associated with OFT progenitor cells (Fig. 1B-E,G-J). In wild-type embryos, *myl7*, *vmhc*, and *nkx2.5* are strongly expressed within differentiated CMs and faintly expressed in an adjacent population of cells presumed to contain SHF-derived OFT progenitors (Fig. 1B,C,L,M) (Lazic and Scott, 2011; Zhou et al., 2011). Cells within this adjacent population also express high levels of *mef2cb* and *ltbp3* (Fig. 1D,E), both of which are thought to mark undifferentiated SHF-derived cells (Lazic and Scott, 2011; Zhou et al., 2011). In SU5402-treated embryos, these markers are substantially downregulated near the arterial pole (Fig. 1G-J), consistent with prior findings (Lazic and Scott, 2011). Similar phenotypes are seen in *fgf8a* mutants (Fig. S1A,B). These data suggest that loss of the OFT in embryos lacking Fgf signaling reflects a requirement for Fgf signaling in promoting the normal formation of OFT progenitor cells.

Cadm4 restricts the number of OFT cardiomyocytes

Since Fgf signaling has a profound effect on development of OFT progenitor cells, we took advantage of SU5402-treated embryos as a platform for discovery of genes involved in OFT progenitor production. We dissociated hearts from SU5402-treated embryos and control siblings and compared their gene expression profiles. Of the differentially expressed genes (Table S1), we were particularly intrigued by *cell adhesion molecule 4 (cadm4)*, which is expressed near the arterial pole in the region where OFT progenitor cells are thought to reside (Fig. 1K-M) and was upregulated in SU5402-treated embryos (Table S1 and Fig. S1C,D).

To investigate the role of *cadm4* during OFT development, we used morpholinos (MOs) to knock down *cadm4* function. Strikingly, we found that embryos injected with these MOs (referred to as *cadm4* morphants) exhibit a dramatically elongated OFT (Fig. 2A-D). Similar effects were seen with each of three non-overlapping MOs (Fig. S2A-D). Using fluorescent reporter transgenes to assess timing of myocardial differentiation (see Experimental Procedures), we determined that the elongated OFT in *cadm4* morphants, like the wild-type OFT, is composed of late-differentiating CMs (Fig. 2J-O), as opposed to containing early-differentiating ventricular cells that were displaced into the OFT. Additionally, we found that elongation of the OFT in *cadm4* morphants is a consequence of containing approximately twice the normal number of late-differentiating CMs (Fig. 2I), rather than simply being the result of altered OFT cell size. As is the case for the wild-type OFT, formation of this expanded OFT requires Fgf signaling: treatment with SU5402 dramatically reduces OFT size in both control and *cadm4* morphant embryos (Fig. S2H-T). In contrast to their excess of OFT CMs, *cadm4* morphants display relatively normal numbers of ventricular and atrial CMs (Fig. 2I); in addition, their heart rate and circulation are

comparable to those of control siblings (Movies S1 and S2). Together, these results indicate an important role for Cadm4 in limiting OFT size.

In complementary experiments, we found that increased levels of *cadm4* expression reduce the size of the OFT. Injection of *cadm4* mRNA resulted in loss of an evident OFT (Fig. 2E-H), and our developmental timing assay revealed that overexpression of *cadm4* reduces the number of late-differentiating CMs (Fig. 2P-R; 32 ± 2 CMs in control embryos ($n=5$) and 17 ± 5 CMs in embryos overexpressing *cadm4* ($n=6$)). Together with our loss-of-function data, these experiments suggest that levels of Cadm4 activity are critical for determining the number of late-differentiating CMs that form the OFT.

Cadm4 delimits the number of OFT progenitor cells

The impact of *cadm4* activity on the size of the OFT could reflect an early influence of *cadm4* on the dimensions of the OFT progenitor pool or a later influence of *cadm4* on the proliferation of OFT CMs. To evaluate early effects of *cadm4* function on the OFT progenitor population, we examined markers of SHF-derived progenitor cells at stages prior to OFT formation. This progenitor population appears substantially enlarged in *cadm4* morphants (Fig. 3A,B,D,E,J; Fig. S3A-H), in contrast to the reduction in progenitors observed when Fgf signaling is deficient (Fig. 1G-J). For example, *mef2cb* expression is visibly expanded in the territory adjacent to the arterial pole of the *cadm4* morphant heart tube (Fig. 3A,B). This expansion is visible as early as 24 hpf (Fig. S3C-F), as are similar expansions of *vmhc* and *ltbp3* expression (Fig. S3A,B,G,H). In addition, *cadm4* morphants display a significantly larger number of cells near the arterial pole that express the transgene *Tg(nkx2.5:ZsYellow)* but do not yet express markers of differentiated myocardium (Fig. 3D,E,J).

In contrast to the expanded population of OFT progenitor cells in *cadm4* morphants, we found that embryos overexpressing *cadm4* possess a notably reduced OFT progenitor population. Overexpression of *cadm4* results in diminished expression of *mef2cb* and *ltbp3* near the arterial pole (Fig. 3A,C; Fig. S2U,W), and *cadm4*-overexpressing embryos exhibit significantly fewer undifferentiated *Tg(nkx2.5:ZsYellow)*-expressing cells in this territory (Fig. 3D,F,J). These decreases in the OFT progenitor population are consistent with the diminutive OFT size observed in *cadm4*-overexpressing embryos (Fig. 2H,R). Furthermore, overexpression of *cadm4* interferes with the ability of elevated Fgf signaling to expand the OFT progenitor population (Fig. S2U-X), highlighting the potency of *cadm4* activity. Together, the converse effects of *cadm4* loss-of-function and gain-of-function suggest an important and early role of Cadm4 in delimiting the pool of OFT progenitor cells.

Although *cadm4* morphants possess an enlarged population of progenitor cells adjacent to the arterial pole (Fig. 3J), the proliferation index of this proximal population, measured by an EdU incorporation assay between 22-24 hpf, is comparable in *cadm4* morphants and control siblings (Fig. 3K). Similarly, as the heart tube lengthens, we have found no evidence of increased proliferation in the differentiated CMs that form the OFT in *cadm4* morphants (Fig. S3L,J). Instead, the number of proliferating OFT CMs appears proportional to the total number of OFT CMs in both *cadm4* morphants and control siblings (Fig. S3K-P). Therefore, it seems that *cadm4* delimits OFT size primarily by delimiting the number of OFT

progenitor cells, rather than by regulating proliferation of OFT progenitors located proximal to the arterial pole or proliferation of differentiated CMs within the OFT. Consistent with this, the near-doubling of the proximal progenitor population in *cadm4* morphants at 24 hpf seems sufficient to account for the comparable increase in OFT size at 48 hpf (Figs. 2I and 3J).

We wondered whether the increased number of OFT progenitor cells in *cadm4* morphants could be the consequence of excess progenitor proliferation prior to their recruitment to the arterial pole. In amniotes, SHF-derived cells that will contribute to the OFT first reside in a distal pharyngeal region where they are maintained in a proliferative state before they proceed to differentiate and move into the heart (Hutson et al., 2010; Tirosh-Finkel et al., 2010; van den Berg et al., 2009). In zebrafish, it has not been shown whether SHF-derived cells travel through a parallel region on their route to the OFT. In this regard, it is interesting to note that our EdU incorporation assays revealed an effect of *cadm4* on the proliferation of a population of *Tg(nkx2.5:ZsYellow)*-expressing cells located distal to the arterial pole (Fig. 3L-Q). In contrast to the *Tg(nkx2.5:ZsYellow)*-expressing cells that are tightly clustered proximal to the heart tube (Fig. 3D-F), the distal population of cells is more dispersed and expresses a lower level of *Tg(nkx2.5:ZsYellow)* (Fig. 3L-N). These traits also distinguish the distal *Tg(nkx2.5:ZsYellow)*-expressing cells from the bilateral clusters of *Tg(nkx2.5:ZsYellow)*-expressing pharyngeal mesendoderm that flank this medially located population (Paffett-Lugassy et al., 2013) (Fig. 3L-N). Our data demonstrate that the number of distal *Tg(nkx2.5:ZsYellow)*-expressing cells is not affected when levels of *cadm4* function are altered (Fig. 3P). However, the proliferation index of this population is significantly increased in *cadm4* morphants and decreased in *cadm4*-overexpressing embryos (Fig. 3Q). Furthermore, photoconversion of distal *Tg(nkx2.5:kaede)*-expressing cells demonstrates that this population contains progenitor cells that contribute to the OFT myocardium (Fig. 3R-Z). Thus, our data suggest that *cadm4* limits the proliferation of OFT progenitor cells prior to their deployment to the arterial pole, thereby restricting the dimensions of the OFT progenitor population.

Cadm4 curtails recruitment of progenitor cells to the arterial pole

In addition to regulating the number of OFT progenitor cells that accumulate at the arterial pole, *cadm4* also appears to regulate the perdurance of progenitor cells in this location. In wild-type embryos, the expression of OFT progenitor markers, such as *mef2cb* and *ltbp3*, declines as OFT CM differentiation proceeds and is ultimately extinguished once differentiation is complete (Lazic and Scott, 2011; Zhou et al., 2011) (Fig. 4A-D). Strikingly, in *cadm4* morphants, expression of *mef2cb* and *ltbp3* is not only spatially expanded but also temporally extended (Fig. 4E-H). Even at 48 hpf, when expression of *mef2cb* and *ltbp3* is nearly undetectable in the wild-type OFT, these genes are still robustly expressed around the arterial pole in *cadm4* morphants (Fig. 4B,D,F,H).

The persistence of OFT progenitor gene expression in *cadm4* morphants suggested the possibility that *cadm4* function is necessary for the normal termination of recruitment of late-differentiating cells to the OFT. Prior studies using a photoconvertible fluorescent reporter transgene to monitor the timing of myocardial differentiation have indicated that

nearly all OFT CMs have undergone differentiation by 36 hpf (Lazic and Scott, 2011). Employing a similar transgene (see Experimental Procedures), we found that *cadm4* morphants continue to add newly-differentiating OFT CMs after 37 hpf (Fig. 4L-N), whereas no new differentiation of OFT CMs was evident after this timepoint in wild-type embryos (Fig. 4I-K). Prolonged addition of OFT CMs was also observed in *cadm4* morphants at even later stages: using both of our assays for timing of differentiation (Figs. 2J-L, 4I-K), we found evidence for initiation of differentiation of OFT CMs in *cadm4* morphants after 48 hpf (Fig. S4).

Together, our data indicate that Cadm4 plays an important role in curtailing the recruitment of progenitor cells into the OFT. Cadm4 is required to limit the number of OFT progenitor cells at the arterial pole, the persistence of OFT progenitor markers, and the duration of the timeframe for OFT CM differentiation. Collectively, these functions of Cadm4 account for its potent impact on restricting the size of the OFT.

DISCUSSION

Our studies reveal an important role for *cadm4* in regulating OFT size. When *cadm4* function is reduced, a surplus of OFT progenitors accumulate at the arterial pole and persist over an extended period of time, creating an abnormally elongated OFT. When *cadm4* levels are elevated, recruitment of OFT progenitors is notably deficient. Thus, our data indicate that downregulation of *cadm4* activity facilitates SHF deployment and promotes the formation of OFT CMs. This discovery provides new insight into the balance between positive and negative influences that determine the number of CMs emerging from the SHF. While several signals are known to stimulate the production of OFT progenitor cells, the function of *cadm4* provides an important demonstration of a pathway that stems the flow of cells from the SHF to the OFT.

The pipeline of OFT CM production involves the specification, proliferation, and maintenance of progenitor cells within the SHF, their subsequent deployment to the arterial pole, and their differentiation into CMs. Our data suggest that *cadm4* limits progenitor deployment by restraining the proliferation of OFT progenitor cells prior to their recruitment to the arterial pole. While the distal *Tg(nkx2.5:ZsYellow)*-expressing cells may not be the only source of OFT progenitors, this scenario could account for the impact of *cadm4* on the rate and duration of OFT progenitor accumulation: excess proliferation and deployment could create an overcrowded pipeline and lead to an overextended timeline for the addition of late-differentiating CMs. Overall, our results are consistent with a model in which levels of Cadm4 activity, regulated by Fgf signaling, act to control the number of OFT progenitor cells that emerge from the SHF. Future studies will be valuable to dissect the precise interface between Fgf signaling and Cadm4 expression and to determine how directly or indirectly Cadm4 influences progenitor proliferation.

Contacts between myelinating Schwann cells and axons are mediated by heterophilic binding between the extracellular domains of glial Cadm4 and axonal Cadm3, and disruption of this interaction leads to reduced myelination (Maurel et al., 2007; Spiegel et al., 2007). Extrapolating from this and other established roles of Cadms, we propose that

Cadm-mediated extracellular interactions in the SHF are crucial for regulating OFT progenitor production. Adhesion between tissue-specific stem cells and their surrounding niches has been shown to be influential in several other contexts (Marthiens et al., 2010), but no such niche has been documented within the SHF. Our studies suggest the possibility that downmodulation of Cadm4 levels alters the interactions between progenitor cells and their niche and influences the dynamics of progenitor proliferation and deployment. Further evaluation of this model will benefit from examining where and when interactions between Cadm family members occur in the distal territory; in this regard, it is intriguing that *cadm2a*, like *cadm4*, is upregulated in SU5402-treated embryos (Table S1). Alternatively, Cadm4 may influence OFT progenitor production through interactions with other signaling pathways; in cell culture, for example, Cadm4 has been shown to interact in *cis* with ErbB receptors (Sugiyama et al., 2013).

Altogether, our data suggest a new paradigm in which extracellular interactions mediated by cell adhesion molecules are essential for controlling the deployment of SHF-derived progenitor cells. It is particularly interesting to consider whether the function of Cadms during SHF deployment is conserved across species. Evaluation of the cardiac role of mammalian Cadms awaits construction of appropriate mouse models (Golan et al., 2013). Our studies also raise the intriguing notion that cell adhesion molecules and even specific *CADM* genes could be relevant to the etiology of human congenital heart disease. Furthermore, modulation of cell adhesion or Cadm function could prove to be a valuable strategy for controlling production of CMs from multipotent cells in vitro.

EXPERIMENTAL PROCEDURES

Protocols for SU5402 treatment, injection, immunofluorescence, in situ hybridization, imaging, microarray analysis, RT-PCR, heat shock, and photoconversion are provided as Supplemental Information.

Zebrafish

We used zebrafish carrying the transgenes *Tg(-5.1myl7:nDsRed2)^{f2}* (Mably et al., 2003), *Tg(myl7:EGFP)^{twu277}* (Huang et al., 2003), *Tg(myl7:DsRed4)^{sk74}* (Garavito-Aguilar et al., 2010), *Tg(myl7:kaede)^{sd22}* (de Pater et al., 2009), *Tg(hsp70:ca-fgfr1)^{pd3}* (Marques et al., 2008), *Tg(nkx2.5:ZsYellow)^{fb7}* (Zhou et al., 2011), and *Tg(nkx2.5:kaede)^{fb9}* (Guner-Ataman et al., 2013), as well as zebrafish carrying the mutation *fgf8a^{ti282a}* (Reifers et al., 2000).

Cell counting and developmental timing assays

We used two complementary developmental timing assays to monitor late-differentiating CMs. For qualitative assessment, we used an established photoconversion protocol in *Tg(myl7:kaede)* embryos (de Pater et al., 2009). Photoconversion of green Kaede protein through exposure to UV light creates red Kaede protein in all differentiated CMs. Subsequently, newly differentiated CMs added since the time of photoconversion will fluoresce green, but not red, and can be distinguished from CMs that were present when photoconversion occurred.

For quantitative assessment, we used a version of an established assay that takes advantage of the temporal difference in maturation of EGFP and DsRed (de Pater et al., 2009). Since DsRed takes longer to mature than EGFP, CMs in *Tg(myl7:EGFP);Tg(myl7:DsRedt4)* embryos show green fluorescence before they show red fluorescence. Newly differentiated CMs will fluoresce green, but not red, and can be distinguished from CMs that differentiated earlier; at 48 hpf, all wild-type OFT CMs fluoresce green, but not red (Fig. 2J-L). To count green, but not red, OFT CMs, we used DAPI to label nuclei and the “spot” function in Imaris to distinguish individual cells in reconstructions of confocal z-stacks. To count ventricular and atrial CMs, we used *Tg(-5.1myl7:nDsRed2)* embryos and the antibody S46, as in our previous work (Marques et al., 2008).

EdU incorporation

We modified established protocols for EdU (5-ethynyl-2'-deoxyuridine) incorporation assays (Cheesman et al., 2011; Mahler et al., 2010). Embryos were incubated in 10mM EdU (Invitrogen) in 0.3X Danieau buffer with 10% DMSO for 20 min on ice. After a series of Danieau washes, embryos were incubated at 28.5 °C until fixation. We then used a Click-iT Imaging kit (Invitrogen) to visualize EdU incorporation. Stained embryos were stored in SlowFade Gold anti-fade reagent with DAPI (Molecular Probes).

To evaluate proliferation of *Tg(nkx2.5:ZsYellow)*-expressing cells (Fig. 3D-Q), we exposed embryos to EdU at 22 hpf and fixed them at 24 hpf. To analyze the proximal population (Fig. 3D-K), we counted the number of *ZsYellow*⁺*MF20*⁻ cells adjacent to the arterial pole. To analyze the distal population (Fig. 3L-Q), we counted the number of *ZsYellow*⁺ cells in a 150 μm wide square positioned 30 μm distal to the heart tube. For each population, we calculated the proliferation index as the percentage of cells that incorporated EdU.

Statistical analysis

To compare data sets, we used Prism software (GraphPad) to perform Student's *t*-test with two-tail distribution. Graphs display mean and standard deviation for each data set.

Supplementary Material

Refer to Web version on PubMed Central for supplementary material.

Acknowledgments

We thank C.G. Burns, I.C. Scott, and P. Washbourne for reagents, D.Y.R. Stainier and W. Driever for EdU advice, and N.C. Chi, S.M. Evans, and members of the Yelon lab for thoughtful input. This work was supported by NIH R01 HL108599 (D.Y.) and an AHA postdoctoral fellowship (X.-X.I.Z.).

REFERENCES

- Biederer T. Bioinformatic characterization of the SynCAM family of immunoglobulin-like domain-containing adhesion molecules. *Genomics*. 2006; 87:139–150. [PubMed: 16311015]
- Biederer T, Sara Y, Mozhayeva M, Atasoy D, Liu X, Kavalali ET, Sudhof TC. SynCAM, a synaptic adhesion molecule that drives synapse assembly. *Science*. 2002; 297:1525–1531. [PubMed: 12202822]

- Buckingham M, Meilhac S, Zaffran S. Building the mammalian heart from two sources of myocardial cells. *Nat Rev Genet.* 2005; 6:826–835. [PubMed: 16304598]
- Cheesman SE, Neal JT, Mittge E, Seredick BM, Guillemin K. Epithelial cell proliferation in the developing zebrafish intestine is regulated by the Wnt pathway and microbial signaling via Myd88. *Proc Natl Acad Sci U S A* 108 Suppl. 2011; 1:4570–4577.
- de Pater E, Clijsters L, Marques SR, Lin YF, Garavito-Aguilar ZV, Yelon D, Bakkens J. Distinct phases of cardiomyocyte differentiation regulate growth of the zebrafish heart. *Development.* 2009; 136:1633–1641. [PubMed: 19395641]
- Dyer LA, Kirby ML. The role of secondary heart field in cardiac development. *Dev Biol.* 2009a; 336:137–144. [PubMed: 19835857]
- Dyer LA, Kirby ML. Sonic hedgehog maintains proliferation in secondary heart field progenitors and is required for normal arterial pole formation. *Dev Biol.* 2009b; 330:305–317. [PubMed: 19361493]
- Garavito-Aguilar ZV, Riley HE, Yelon D. Hand2 ensures an appropriate environment for cardiac fusion by limiting Fibronectin function. *Development.* 2010; 137:3215–3220. [PubMed: 20724450]
- Golan N, Kartvelishvily E, Spiegel I, Salomon D, Sabanay H, Rechav K, Vainshtein A, Frechter S, Maik-Rachline G, Eshed-Eisenbach Y, et al. Genetic deletion of *Cadm4* results in myelin abnormalities resembling charcot-marie-tooth neuropathy. *J Neurosci.* 2013; 33:10950–10961. [PubMed: 23825401]
- Guner-Ataman B, Paffett-Lugassy N, Adams MS, Nevis KR, Jahangiri L, Obregon P, Kikuchi K, Poss KD, Burns CE, Burns CG. Zebrafish second heart field development relies on progenitor specification in anterior lateral plate mesoderm and *nkx2.5* function. *Development.* 2013; 140:1353–1363. [PubMed: 23444361]
- Hami D, Grimes AC, Tsai HJ, Kirby ML. Zebrafish cardiac development requires a conserved secondary heart field. *Development.* 2011; 138:2389–2398. [PubMed: 21558385]
- Huang CJ, Tu CT, Hsiao CD, Hsieh FJ, Tsai HJ. Germ-line transmission of a myocardium-specific GFP transgene reveals critical regulatory elements in the cardiac myosin light chain 2 promoter of zebrafish. *Dev Dyn.* 2003; 228:30–40. [PubMed: 12950077]
- Hutson MR, Zeng XL, Kim AJ, Antoon E, Harward S, Kirby ML. Arterial pole progenitors interpret opposing FGF/BMP signals to proliferate or differentiate. *Development.* 2010; 137:3001–3011. [PubMed: 20702561]
- Ilagan R, Abu-Issa R, Brown D, Yang YP, Jiao K, Schwartz RJ, Klingensmith J, Meyers EN. *Fgf8* is required for anterior heart field development. *Development.* 2006; 133:2435–2445. [PubMed: 16720880]
- Kelly RG. The second heart field. *Curr Top Dev Biol.* 2012; 100:33–65. [PubMed: 22449840]
- Lazic S, Scott IC. *Mef2cb* regulates late myocardial cell addition from a second heart field-like population of progenitors in zebrafish. *Dev Biol.* 2011; 354:123–133. [PubMed: 21466801]
- Mably JD, Mohideen MA, Burns CG, Chen JN, Fishman MC. *heart of glass* regulates the concentric growth of the heart in zebrafish. *Curr Biol.* 2003; 13:2138–2147. [PubMed: 14680629]
- Mahler J, Filippi A, Driever W. *DeltaA/DeltaD* regulate multiple and temporally distinct phases of notch signaling during dopaminergic neurogenesis in zebrafish. *J Neurosci.* 2010; 30:16621–16635. [PubMed: 21148001]
- Marques SR, Lee Y, Poss KD, Yelon D. Reiterative roles for FGF signaling in the establishment of size and proportion of the zebrafish heart. *Dev Biol.* 2008:397–406. [PubMed: 18639539]
- Marthiens V, Kazanis I, Moss L, Long K, Ffrench-Constant C. Adhesion molecules in the stem cell niche—more than just staying in shape? *J Cell Sci.* 2010; 123:1613–1622. [PubMed: 20445012]
- Maurel P, Einheber S, Galinska J, Thaker P, Lam I, Rubin MB, Scherer SS, Murakami Y, Gutmann DH, Salzer JL. Nectin-like proteins mediate axon Schwann cell interactions along the internode and are essential for myelination. *J Cell Biol.* 2007; 178:861–874. [PubMed: 17724124]
- Neeb Z, Lajiness JD, Bolanis E, Conway SJ. Cardiac outflow tract anomalies. *Wiley Interdiscip Rev Dev Biol.* 2013; 2:499–530. [PubMed: 24014420]
- Paffett-Lugassy N, Singh R, Nevis KR, Guner-Ataman B, O'Loughlin E, Jahangiri L, Harvey RP, Burns CG, Burns CE. Heart field origin of great vessel precursors relies on *nkx2.5*-mediated vasculogenesis. *Nat Cell Biol.* 2013; 15:1362–1369. [PubMed: 24161929]

- Park EJ, Ogden LA, Talbot A, Evans S, Cai CL, Black BL, Frank DU, Moon AM. Required, tissue-specific roles for Fgf8 in outflow tract formation and remodeling. *Development*. 2006; 133:2419–2433. [PubMed: 16720879]
- Park EJ, Watanabe Y, Smyth G, Miyagawa-Tomita S, Meyers E, Klingensmith J, Camenisch T, Buckingham M, Moon AM. An FGF autocrine loop initiated in second heart field mesoderm regulates morphogenesis at the arterial pole of the heart. *Development*. 2008; 135:3599–3610. [PubMed: 18832392]
- Pietri T, Easley-Neal C, Wilson C, Washbourne P. Six cadm/SynCAM genes are expressed in the nervous system of developing zebrafish. *Dev Dyn*. 2008; 237:233–246. [PubMed: 18095341]
- Prall OW, Menon MK, Solloway MJ, Watanabe Y, Zaffran S, Bajolle F, Biben C, McBride JJ, Robertson BR, Chaulet H, et al. An Nkx2-5/Bmp2/Smad1 negative feedback loop controls heart progenitor specification and proliferation. *Cell*. 2007; 128:947–959. [PubMed: 17350578]
- Reifers F, Walsh EC, Leger S, Stainier DY, Brand M. Induction and differentiation of the zebrafish heart requires fibroblast growth factor 8 (fgf8/acerebellar). *Development*. 2000; 127:225–235. [PubMed: 10603341]
- Rochais F, Mesbah K, Kelly RG. Signaling pathways controlling second heart field development. *Circ Res*. 2009; 104:933–942. [PubMed: 19390062]
- Ryckebusch L, Wang Z, Bertrand N, Lin SC, Chi X, Schwartz R, Zaffran S, Niederreither K. Retinoic acid deficiency alters second heart field formation. *Proc Natl Acad Sci U S A*. 2008; 105:2913–2918. [PubMed: 18287057]
- Sirbu IO, Zhao X, Duester G. Retinoic acid controls heart anteroposterior patterning by down-regulating *Isl1* through the Fgf8 pathway. *Dev Dyn*. 2008; 237:1627–1635. [PubMed: 18498088]
- Sorrell MR, Waxman JS. Restraint of Fgf8 signaling by retinoic acid signaling is required for proper heart and forelimb formation. *Dev Biol*. 2011; 358:44–55. [PubMed: 21803036]
- Spiegel I, Adamsky K, Eshed Y, Milo R, Sabanay H, Sarig-Nadir O, Horresh I, Scherer SS, Rasband MN, Peles E. A central role for *Necl4* (SynCAM4) in Schwann cell-axon interaction and myelination. *Nat Neurosci*. 2007; 10:861–869. [PubMed: 17558405]
- Sugiyama H, Mizutani K, Kurita S, Okimoto N, Shimono Y, Takai Y. Interaction of *Necl-4/CADM4* with *ErbB3* and integrin $\alpha6\beta4$ and inhibition of *ErbB2/ErbB3* signaling and hemidesmosome disassembly. *Genes Cells*. 2013; 18:519–528. [PubMed: 23611113]
- Tirosh-Finkel L, Zeisel A, Brodt-Ivenshitz M, Shamaï A, Yao Z, Seger R, Domany E, Tzahor E. BMP-mediated inhibition of FGF signaling promotes cardiomyocyte differentiation of anterior heart field progenitors. *Development*. 2010; 137:2989–3000. [PubMed: 20702560]
- van den Berg G, Abu-Issa R, de Boer BA, Hutson MR, de Boer PA, Soufan AT, Ruijter JM, Kirby ML, van den Hoff MJ, Moorman AF. A caudal proliferating growth center contributes to both poles of the forming heart tube. *Circ Res*. 2009; 104:179–188. [PubMed: 19059840]
- Watanabe Y, Miyagawa-Tomita S, Vincent SD, Kelly RG, Moon AM, Buckingham ME. Role of mesodermal FGF8 and FGF10 overlaps in the development of the arterial pole of the heart and pharyngeal arch arteries. *Circ Res*. 2010; 106:495–503. [PubMed: 20035084]
- Witzel HR, Jungblut B, Choe CP, Crump JG, Braun T, Dobrev G. The LIM protein *Ajuba* restricts the second heart field progenitor pool by regulating *Isl1* activity. *Dev Cell*. 2012; 23:58–70. [PubMed: 22771034]
- Zhou Y, Cashman TJ, Nevis KR, Obregon P, Carney SA, Liu Y, Gu A, Mosimann C, Sondalle S, Peterson RE, et al. Latent TGF-beta binding protein 3 identifies a second heart field in zebrafish. *Nature*. 2011; 474:645–648. [PubMed: 21623370]

Highlights

Cadm4 restricts the number of outflow tract cardiomyocytes.

Cadm4 delimits the number of outflow tract progenitor cells.

Cadm4 curtails the recruitment of progenitor cells to the arterial pole.

Cell adhesion may be critical to restrain outflow tract progenitor deployment.

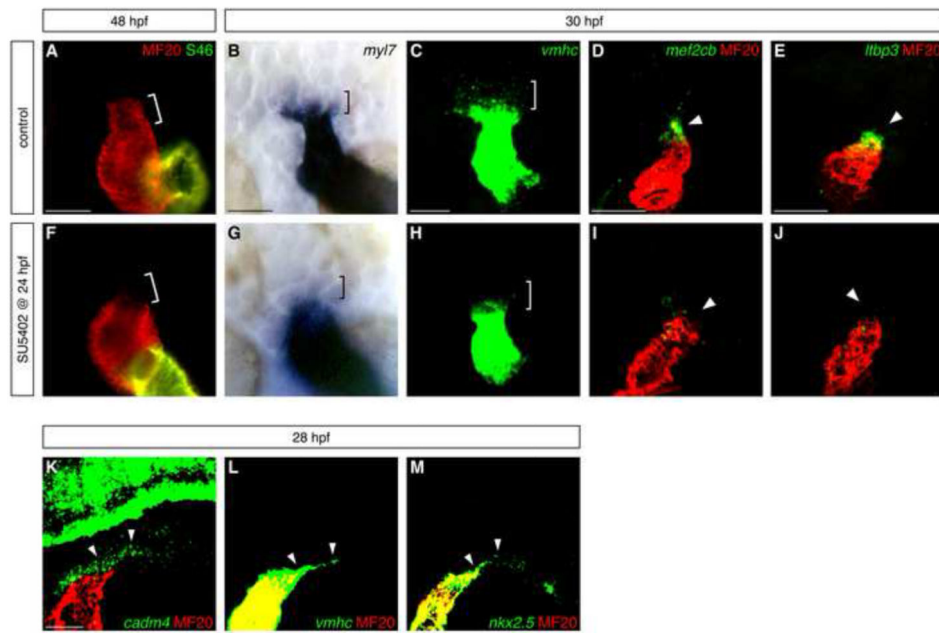


Figure 1. Fgf signaling promotes formation of OFT progenitor cells

(A,F) Hearts at 48 hpf, frontal views, arterial pole up, stained with MF20 (red) and S46 (green) antibodies to visualize the OFT (red, bracket), ventricle (red), and atrium (yellow). The OFT is morphologically evident in control DMSO-treated embryos (A) and absent in embryos treated with 10 μ M SU5402 from 24-48 hpf (F).

(B-E,G-J) In situ hybridization highlights the presumed OFT progenitor cells adjacent to the arterial pole at 30 hpf. Dorsal views (B,C,G,H) and lateral views (D,E,I,J), arterial pole up; (C-E,H-J) partial reconstructions of confocal z-stacks. The presumed OFT progenitors (brackets) express low levels of *myl7* (blue, B) and *vmhc* (green, C); very few of these cells are found in embryos treated with SU5402 from 24-30 hpf (G,H). Expression of *mef2cb* (green, D) and *ltbp3* (green, E) is visible in the progenitor cells (arrowheads) residing next to the differentiated myocardium of the heart tube (MF20, red); this population is barely detectable in SU5402-treated embryos (I,J).

(K-M) Fluorescent in situ hybridization shows that *cadm4* (green, K) is expressed in the region where OFT progenitor cells are thought to reside (arrowheads), as well as in neuronal tissues as previously reported (Pietri et al., 2008). *vmhc* (green, L) and *nkx2.5* (green, M) are expressed at low levels within the same region (arrowheads), as well as at high levels throughout the heart tube. Differentiated myocardium is marked by MF20 (red); partial reconstructions of lateral views at 28 hpf.

Scale bars: 50 μ m.

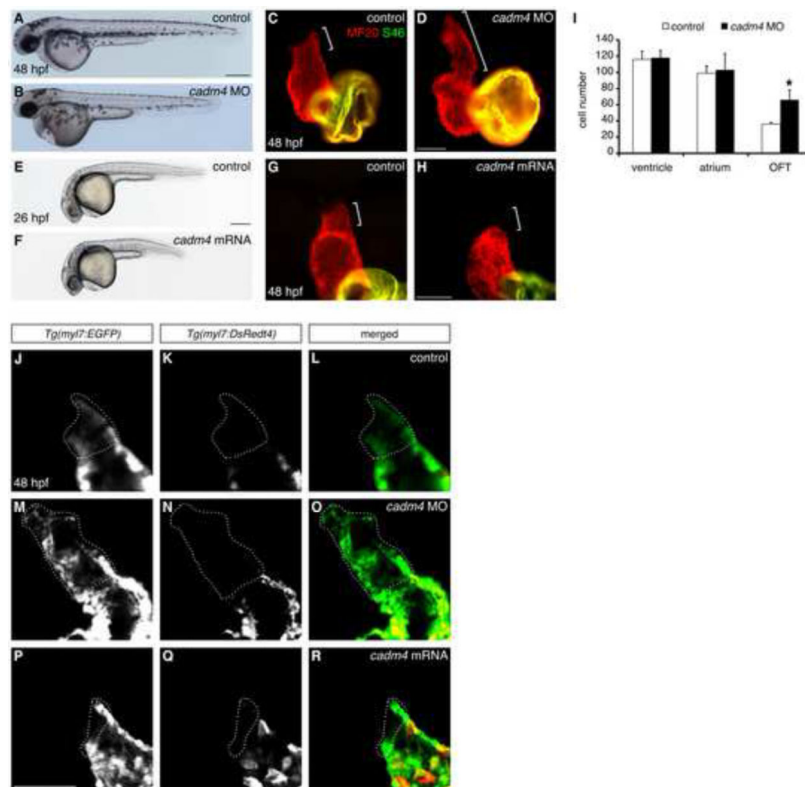


Figure 2. Cadm4 activity limits OFT size

(A-D) Reduced *cadm4* function results in an enlarged OFT. (A,B) Lateral views of embryos at 48 hpf. Injection of an anti-*cadm4* MO (B) does not disrupt general embryonic morphology. (C,D) Hearts at 48 hpf, as in Fig. 1A. Compared to the normal length of the OFT (bracket, C) in control sibling embryos, the OFT in *cadm4* morphants is abnormally elongated (bracket, D).

(E-H) Elevated levels of *cadm4* function result in reduced OFT size. (E,F) Lateral views of embryos at 26 hpf. Injection of *cadm4* mRNA (F) causes slight shortening of the body axis. (G,H) Hearts at 48 hpf, as in (C). Rather than exhibiting normal OFT size (bracket, G), embryos injected with *cadm4* mRNA exhibit very little OFT tissue (bracket, H).

(I) Number of ventricular, atrial, and OFT CMs in control and *cadm4* morphant hearts at 48 hpf. While the numbers of ventricular and atrial CMs are unaffected in *cadm4* morphants, the OFT in *cadm4* morphants has more CMs than the OFT in control siblings ($p < 0.0005$, asterisk; $n = 5$).

(J-R) Single confocal slices through *Tg(myf7:EGFP);Tg(myf7:DsRed4)* hearts at 48 hpf, arterial pole up. These transgenes can distinguish early-differentiating CMs (EGFP and DsRed) from late-differentiating CMs (EGFP only, dotted outlines). Compared to controls (J-L), *cadm4* morphants have an excess of late-differentiating CMs (M-O), and embryos injected with *cadm4* mRNA have a deficit of late-differentiating CMs (P-R).

Scale bars in (A,E) are 300 μ m. Scale bars in (D,H,P) are 50 μ m.

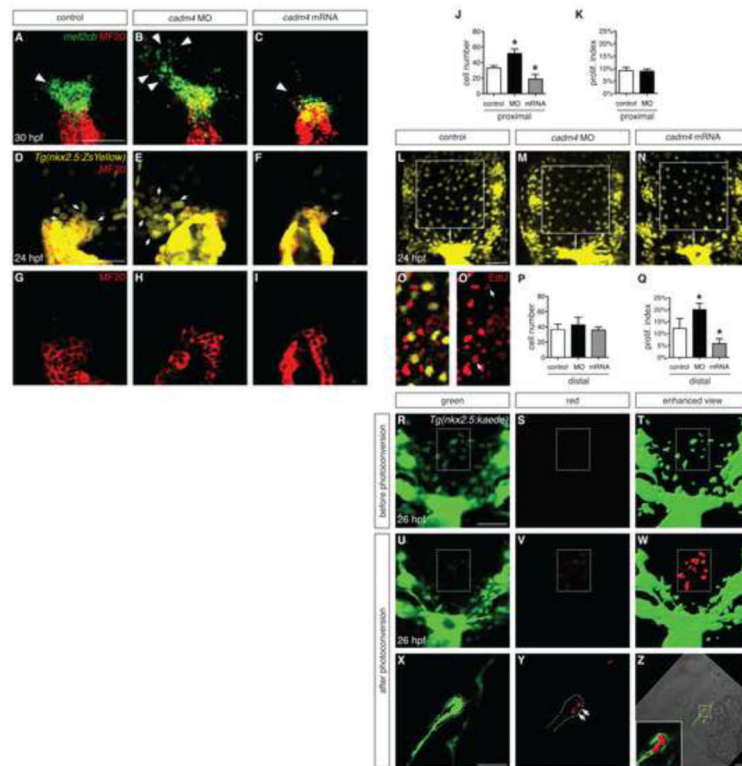


Figure 3. *Cadm4* limits formation of OFT progenitor cells

(A-C) In situ hybridization shows expression of *mef2cb* (green) in progenitor cells adjacent to the differentiated myocardium (MF20, red); partial reconstructions of dorsal views at 30 hpf, arterial pole up. In comparison to control embryos (A), this progenitor population (arrowheads) is expanded in *cadm4* morphants (B) and reduced in embryos overexpressing *cadm4* (C).

(D-I) Partial reconstructions of dorsal views of arterial poles expressing *Tg(nkx2.5:ZsYellow)* (yellow, D-F) at 24 hpf; MF20 (red, D-I) marks differentiated CMs. In control embryos (D,G), undifferentiated progenitor cells (yellow, not red; arrows indicate examples) cluster in a proximal region adjacent to the arterial pole. This population is expanded in *cadm4* morphants (E) and reduced in embryos overexpressing *cadm4* (F).

(J) Number of *ZsYellow*⁺MF20⁻ OFT progenitor cells in the proximal region at 24 hpf in control embryos, *cadm4* morphants, and embryos injected with *cadm4* mRNA; asterisks indicate statistically significant differences from controls ($p < 0.0001$; $n = 9-14$). Comparable progenitor surpluses resulted from injection of either of two non-overlapping MOs (52 ± 6 cells, ATG MO1 ($n = 14$); 58 ± 6 cells, splice MO ($n = 7$)). (K) Proliferation indexes are comparable for the proximal OFT progenitor cells in control embryos and *cadm4* morphants. (L-N) Partial reconstructions of dorsal views of the region near the arterial pole in embryos expressing *Tg(nkx2.5:ZsYellow)* at 24 hpf; images were captured with a higher gain than (D-F). Squares indicate the region defined as distal in representative control (L), *cadm4* morphant (M), and *cadm4*-overexpressing (N) embryos.

(O-O') EdU incorporation (red) in an embryo expressing *Tg(nkx2.5:ZsYellow)* (yellow); EdU is visible in at least two *Tg(nkx2.5:ZsYellow)*-expressing cells (arrows) in this representative slice.

(P) Numbers of *Tg(nkx2.5:ZsYellow)*-expressing cells in the distal regions of control, *cadm4* morphant, and *cadm4*-overexpressing embryos are similar (n=7-12).

(Q) The proliferation index is increased in the distal *Tg(nkx2.5:ZsYellow)*-expressing cells in *cadm4* morphants (p<0.0005, asterisk) and is decreased in the same population in *cadm4*-overexpressing embryos (p<0.0001, asterisk).

(R-W) Single slices show dorsal views near the arterial pole in a representative *Tg(nkx2.5:kaede)* embryo at 26 hpf, before (R-T) and after (U-W) photoconversion of a portion of the distal region (rectangle) containing approximately 10 *Tg(nkx2.5:kaede)*-expressing cells (green in T, red in W). Enhanced views (T,W) were generated using the “surface” function in Imaris to highlight cells expressing low levels of *Tg(nkx2.5:kaede)*.

(X-Z) Single slices show lateral views of *Tg(nkx2.5:kaede)* expression in the heart at 30 hpf and indicate that 3-4 of the photoconverted cells (red, arrows) have become OFT CMs. Dots (X,Y) outline ventral wall of the forming OFT. Bright-field image and magnified inset (Z) show the incorporation of red photoconverted cells within the green OFT myocardium.

Similar results were obtained in 4 independent embryos.

Scale bars: 50 μ m.

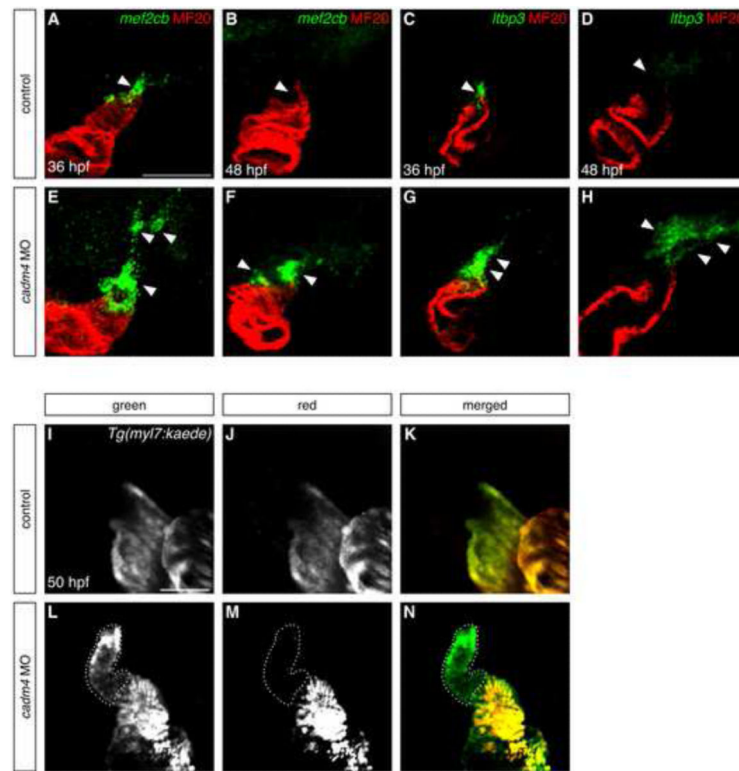


Figure 4. Cadm4 curtails addition of late-differentiating cells to the arterial pole
 (A-H) Expression of *mef2cb* (A,B,E,F) and *ltbp3* (C,D,G,H) juxtaposed with staining of differentiated myocardium (as in Fig. 1D,E) at 36 (A,C,E,G) and 48 (B,D,F,H) hpf; partial reconstructions (A,B,E,F) or single slices (C,D,G,H) of lateral views. (A-D) In control embryos, expression of both genes (arrowheads) becomes extinguished as OFT differentiation reaches completion. (E-H) In contrast, expression of both genes (arrowheads) is expanded and prolonged in *cadm4* morphants.
 (I-N) Single slices of lateral views of *Tg(myl7:kaede)*-expressing hearts at 50 hpf, following photoconversion at 37 hpf. Comparison of green fluorescence (I,L) and red fluorescence (J,M) reveals the presence of late-differentiating cells (green, not red; dotted outlines). (I-K) Control embryos do not exhibit addition of late-differentiating cells between 37-50 hpf (n=34). (L-N) In contrast, *cadm4* morphants exhibit a population of green, but not red, OFT cells that initiated differentiation during this timeframe (n=42). Scale bars: 50 μ m.